A Cucurbit[6]uril Analogue: Host Properties Monitored by Fluorescence Spectroscopy

Brian D. Wagner,*,† Patricia G. Boland,† Jason Lagona,‡ and Lyle Isaacs*,‡

Department of Chemistry, University of Prince Edward Island, Charlottetown, PE, C1A 4P3, Canada, and Department of Chemistry and Biochemistry, University of Maryland, College Park, Maryland 20742

Received: December 10, 2004; In Final Form: February 11, 2005

This paper describes the host properties of a new cucurbit[6]uril analogue, studied by fluorescence and ^{1}H NMR spectroscopy. This host has an elongated cavity with oval-shaped portals. It is intrinsically fluorescent, and more importantly, this fluorescence is sensitive to guest encapsulation, allowing for the study of the inclusion of nonfluorescent guests by fluorescence spectroscopy. In the case of benzene as guest, significant enhancement of the cucurbit[6]uril analogue host fluorescence was observed upon addition of benzene; this allowed for the determination of the binding constant for 1:1 host−guest complexation, yielding a value of $K = 6900 \pm 1100$ M^{-1}. This complexation was also studied by ^{1}H NMR, yielding a similar value of $K = 8980 \pm 500$ M^{-1}. The binding of a much larger guest, the dye Nile Red, was also studied, but in this case using guest fluorescence. Significant suppression of the Nile Red fluorescence was observed upon 1:1 complexation with the cucurbit[6]uril analogue, with an extremely large binding constant of $8.2 \pm 0.5 \times 10^6$ M^{-1}, indicating a very strong host−guest interaction and an excellent size and shape match. In both cases, binding was much stronger than in the case of the same guests with cucurbit[6]uril itself, and in the case of Nile Red, binding was also much stronger than with modified β- or γ-cyclodextrins. This is partly a result of the partial aromatic nature of the host walls, which allow for $\pi-\pi$ interactions not possible in cucurbiturils or cyclodextrins. The ability to study its inclusion complexes using either host or guest fluorescence, and the very high binding constants observed, illustrates the versatility and potential usefulness of this new host compound.

1. Introduction

Since the elucidation of the molecular structure of cucurbit[6]uril (CB[6]) by Mock in 1981 (76 years after its first synthesis by Behrend in 1905), many research laboratories have published results on the recognition properties of this unique receptor including Mock,[1−4] Buschmann,[5,6] and Kim.[7−9] CB[6] has the ability to encapsulate several different types of guests in its hydrophobic cavity because of a combination of noncovalent interactions including the hydrophobic effect, ion−dipole interactions, and hydrogen bonding. The selectivity of CB[6] is due to the rigidity of the macrocycle which allows for guests of proper size, shape, and functionality to form thermodynamically stable complexes ($K_d < 1$ μM). We recently reported a new class of macrocyclic hosts, CB[n] analogues, based on glycoluril and bis-phthalhydrazide.[10] The recognition properties of these CB[n] analogues differ from those of CB[6] because two aromatic walls have been incorporated into the macrocycle which (1) defines a cavity lined by aromatic rings which should impart a high selectivity for aromatic and cationic guests, (2) allows for detection by UV−vis, and (3) allows for detection by fluorescence. In this paper, we discuss the CB[6] analogue **1** (R = CO_2H) and its molecular recognition properties on the basis of results obtained from fluorescence spectroscopy.

The detection of CB[6] encapsulating guests was first reported using alkylammonium ions on the basis of experimental data from ^{1}H NMR,[11] UV−vis,[12] and calorimetry.[13] Since then, the binding of CB[6] to alkali metal cations,[14] amino acids, amino alcohols,[15] and amino azabenzenes[16] has been reported. In contrast, a limited number of investigators have used fluorescence experiments to determine the binding constants of certain guests toward CB[6]. Because CB[6] is not fluorescent, these studies from the groups of Wagner,[17−20] Kim,[21,22] Buschmann,[23] and Nau[24] employ fluorescent guests. For example, Wagner and Buschmann independently reported fluorescence experiments using a mixture of 1-anilinonaphthalene-8-sulfonate (1,8-ANS) and CB[6] in the solid state. These experiments showed an enhancement in the fluorescence of 1,8-ANS when bound to CB[6].

Figure 2 shows the X-ray crystal structure of compound **2** which confirms the elongated shape of the CB[6] analogues, with dimensions of $5.90 \times 11.15 \times 6.92$ Å, compared to the cylindrically shaped CB[6]. These CB[n] analogues are expected to combine the advantageous features—tight binding, high selectivity, and unusual dynamics—of two important classes of host molecules, namely, CB[n] and cyclophanes.[25−27] Since these CB[6] analogues possess fluorescent properties, our group envisioned using compounds as hosts molecules to study the binding properties of a wide variety of guest molecules including alkylamines, arylamines, dyes, amino acids, peptides, and nucleotides.

The incorporation of the phthalhydrazide walls into the macrocycle gives the ability for detection by long wavelength UV−vis and fluorescence spectroscopy. In addition to ion−dipole interactions and the hydrophobic effect, complexes of the CB[6] analogue also benefit from $\pi-\pi$ interactions with guests containing aromatic rings. Aside from the different chemical functionality of the walls of the CB[6] analogue relative to CB[6], the CB[6] analogue also possesses a very different shape. Its cavity is oval which imparts selectivity for longer, flatter aromatic guests relative to CB[n] which prefer more spherical guests. Herein, we report the binding of CB[6]

* Corresponding authors. B.D.W.: tel: 1-902-628-4351; fax: 1-902-566-0632; e-mail: bwagner@upei.ca. L.I.: tel: 1-301-405-1884; fax: 1-301-314-9121; e-mail: lisaacs@umd.edu.

† University of Prince Edward Island.

‡ University of Maryland.

10.1021/jp044369c CCC: $30.25
Published on Web 03/22/2005

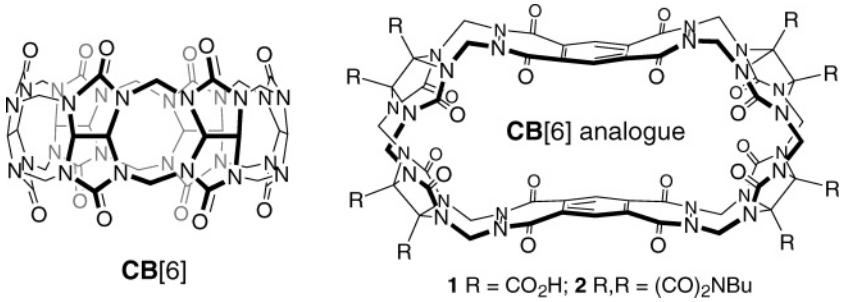

Figure 1. CB[6] and CB[6] analogues **1** and **2**.

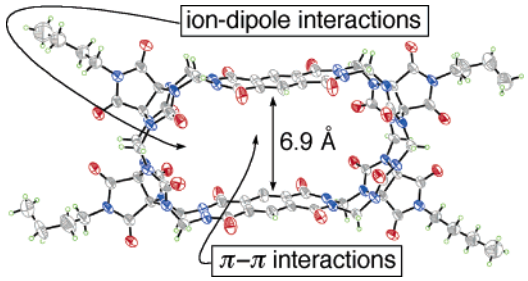

Figure 2. X-ray crystal structure of **2** (C-gray, H-green, N-blue, O-red).

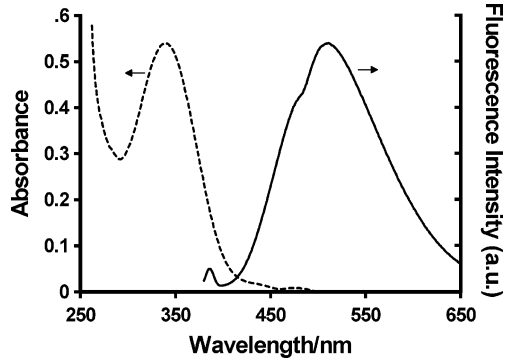

Figure 3. Absorption (---) and fluorescence (——) spectrum of 30 μM **1** in acetate buffer.

analogue octacarboxylic acid (**1**) toward benzene and Nile Red in a sodium acetate buffer (pH 4.74, 50 mM) monitored using fluorescence spectroscopy.

2. Experimental Section

Materials. Cucurbit[6]uril analogue **1** was synthesized and purified according to published methods.[10] The following compounds were purchased from the indicated sources and used as received: benzene (BDH), sodium acetate (Mallinckrodt), acetic acid (Fisher), Nile Red (Aldrich).

Solution Preparation. All solutions were prepared in 50 mM sodium acetate/acetic acid buffer (pH 4.74, 50 mM). In the benzene study, a 30 μM stock solution of **1** was prepared, and the appropriate volume of benzene was added to 3.00-mL aliquots of this stock solution using a 10-μL syringe. In the Nile Red study, a saturated Nile Red solution was prepared in the acetate buffer. The appropriate amount of **1** was weighed into 5-mL glass vials and then dissolved by adding 3.00 mL of the Nile Red stock solution.

Fluorescence Spectroscopy. All absorption and fluorescence measurements were performed on solutions in 1 cm^2 quartz cuvettes, at 22 ± 1 °C. Absorption spectra were measured on a Cary 50 Bio UV−Visible spectrophotometer. Fluorescence spectra were measured on a Photon Technology International LS-100 luminescence spectrometer, with excitation and emission monochromator band-passes set at 3 nm. In the cucurbit[6]uril analogue **1** fluorescence, an excitation wavelength of 340 nm was used (360 nm for the benzene titration study), whereas 560 nm was used for Nile Red fluorescence. The fluorescence quantum yield of **1** was determined using the relative method with 9,10-diphenylanthracene in cyclohexane as the standard ($\phi_F = 0.90$).[28] The fluorescence enhancement F/F_o was determined at each host (or guest) concentration as the ratio of the integrated fluorescence spectrum (intensity vs wavenumber) in the presence of the host (or guest) to that in its absence. Time-resolved fluorescence was measured on a Photon Technology International TimeMaster fluorescence lifetime spectrometer, which uses the stroboscopic technique.[29] Decay curves were analyzed using the instrument deconvolution software and were fit successfully to single-exponential decay functions.

^{1}H NMR Spectroscopy. All spectra were recorded on a spectrometer operating at 400 MHz for ^{1}H and are referenced to external $(CH_3)_3SiCD_2CD_2CO_2H$ ($\delta = 0.0$ ppm). The temperature was calibrated using the separation of the resonances of $HOCH_2CH_2OH$ and controlled at 22 ± 1 °C using a Bruker Eurotherm module. The chemical shifts of the host were monitored as a function of added benzene concentration and the tabulated values of chemical shift versus concentration were used to determine values of K by nonlinear least-squares analysis.

Computational Results. Calculations were performed using Spartan '02 v. 1.0.7 for Macintosh employing the MMFF force field.

3. Results and Discussion

3.1. Fluorescence Properties of Cucurbit[6]uril Analogue 1. The UV−vis absorption spectrum of **1** was reported previously[10] and consists of a broad, featureless band with a maximum at 340 nm, which extends out to ca. 450 nm. Figure 3 shows both the absorption and the fluorescence spectrum of a 30 μM solution of cucurbit[6]uril analogue **1** in acetate buffer. The fluorescence spectrum is also broad and featureless, with a maximum emission wavelength of 510 nm. As can be seen from Figure 3, this molecule thus exhibits a very large Stokes shift, with a value of 9800 cm^{-1}. This indicates that there is significant geometry change in the equilibrium configuration of the excited state relative to that of the ground state; this could include both conformational changes and solvent reorientation.[30]

The fluorescence lifetime τ_F was measured to be 1.4 ± 0.4 ns. A low fluorescence quantum yield ϕ_F of 0.0023 was measured. Thus, the fluorescence of cucurbit[6]uril analogue **1** is relatively weak and short-lived. The values of the rate constants for radiative (k_R) and total nonradiative (k_{NR}) decay of the S_1 of cucurbit[6]uril analogue **1** can be determined from the measured values of τ_F ($=1/\{k_R + k_{NR}\}$) and ϕ_F ($=k_R/\{k_R + k_{NR}\}$); this analysis gives $k_R = 1.8 \times 10^6$ s^{-1} and $k_{NR} = 7.7 \times 10^8$ s^{-1}. Thus, the low quantum yield and short lifetime of the S_1 state is a result of relatively fast nonradiative decay.

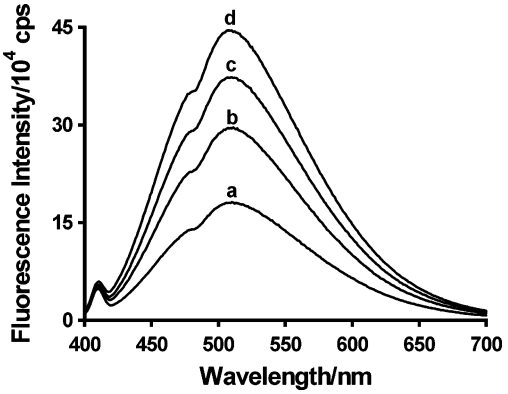

Figure 4. Fluorescence spectrum of 25 μM **1** in acetate buffer in the (a) absence and (b−d) presence of benzene: (b) 0.125 mM; c: 0.50 mM; d: 10 mM.

3.2. Effect of Benzene Inclusion on Cucurbit[6]uril Analogue 1 Fluorescence. The fact that cucurbit[6]uril analogue **1** is fluorescent presents the possibility of fluorescence studies of its host properties even in the case of nonfluorescent guests, a possibility that does not exist for nonfluorescent hosts such as cyclodextrins and the CB[n] family. This opportunity is dependent on the extent to which the fluorescence of cucurbit-[6]uril analogue **1** is sensitive to the presence of guests included in its cavity. Figure 4 shows the fluorescence spectrum of **1** as a function of added benzene recorded at an excitation wavelength of 330 nm where CB[6] analogue absorbs but where benzene does not absorb. A significant enhancement of the fluorescence of **1** is observed, probably because of inclusion of the benzene within the cavity of **1**. The total fluorescence enhancement (F/F_o) can be calculated as the ratio of the integrated fluorescence spectrum (plotted in terms of wavenumber) of **1** in the presence and absence of benzene; at 10 mM benzene, an enhancement of a factor 2.40 is obtained. There is no observed shifting of the position of the spectral maximum: $\lambda_{F,max} = 510 \pm 2$ nm at all concentrations of benzene.

Thus, cucurbit[6]uril analogue **1** fluorescence is indeed sensitive to inclusion of guest species within its cavity. Since the fluorescence wavelength maximum is unaffected by inclusion, the observed enhancement is not a result of a change in the energy of the S_1 state relative to the ground state upon inclusion. Since enhancement is observed, this is also not a result of quenching of the host fluorescence by the included benzene. We propose that this sensitivity is a result of changes in the conformation of the host molecule upon inclusion of the benzene guest and that the new conformation results in either an increase in the radiative decay rate or, more likely, a decrease in the very large nonradiative decay rate, resulting in the observed increased fluorescence quantum yield. Figure 5a shows the geometry obtained from molecular mechanics calculations (MMFF) of the **1**·C_6H_6 complex. The C_6H_6 molecule is complexed on one side of the macrocycle; the remaining volume is insufficient to host a second C_6H_6 molecule.

In the enhancement of guest (G) fluorescence upon addition of a nonfluorescent host (H) as a result of the formation of 1:1 host:guest inclusion complexes ({H:G}), the measured enhancement depends on the added host concentration according to the equation[31,32]

$$F/F_o = 1 + (F_\infty/F_o - 1)\frac{[H]K}{(1 + [H]K)} \quad (1)$$

where F_∞/F_o is the enhancement when 100% of the fluorescent host molecules are complexed, and K is the equilibrium binding constant for the 1:1 complexation

$$H + G \rightleftharpoons \{H:G\} \quad (2)$$

$$K = \frac{[\{H:G\}]}{[H][G]} \quad (3)$$

Confirmation of 1:1 complexation (and hence the applicability of eq 1) can be obtained from the double reciprocal plot of $1/(F/F_o - 1)$ versus $1/[H]$; this will be linear if only 1:1 complexation is occurring but will be nonlinear if higher-order complexes also form.

Analysis of the derivation of eq 1 (given in ref 31) shows that it does not in fact matter whether it is the guest or host fluorescence being measured (the host and guest are interchangeable in eqs 2 and 3, since this is for 1:1 complexation). Thus, eq 1 can also be applied to the enhancement of cucurbit-[6]uril analogue **1** host fluorescence by the added guest benzene and can be used to determine the binding constant K from the fluorescence titration data of F/F_o for a fixed concentration of **1** as a function of benzene concentration. In fact, there have been a few previous reports of the extraction of binding constants from the fluorescence of hosts titrated with nonfluorescent guests, including that of Fabbrizzi et al. for a fluorescent bistren cage compound[33] and that of Nolte and co-workers for a luminescent ruthenium complex with attached cyclodextrin binding sites.[34]

Figure 6a shows the enhancement of cucurbit[6]uril analogue **1** fluorescence as function of added benzene. The inset shows the linear double reciprocal plot ($r = 0.992$), which confirms the 1:1 stoichiometry of the complex. The solid line shows the excellent fit to eq 1, in this case giving $K = 6700$ M^{-1} and $F_\infty/F_o = 2.43$. Four such trials were performed, yielding the average values of $K = 6900 \pm 1100$ M^{-1} and $F_\infty/F_o = 2.40 \pm 0.04$.

The binding of benzene by **1** could also be monitored by ^{1}H NMR spectroscopy. Figure 6b shows a plot of chemical shift of the four equivalent aryl H atoms in **1** versus the benzene concentration observed during the titration of a solution of **1** (100 μM) with benzene. The data are well described by a simple 1:1 host:guest binding model (solid line) with $K = 8980 \pm 500$ M^{-1}, in reasonable agreement with the value of 6700 M^{-1} obtained by fluorescence. The 1:1 stoichiometry was confirmed by Job plot analysis (not shown). Furthermore, the upfield chemical shift observed for **1**·benzene ($\Delta\delta = 0.185$) suggests that benzene is binding within the cavity of **1** resulting in an anisotropic shielding effect on these four aromatic protons. Although we believe that the geometry depicted in Figure 5a represents a snapshot of the **1**·benzene complex, the ^{1}H NMR spectrum of **1**·C_6H_6 indicates time-averaged C_{2v}-symmetry on the NMR time scale which indicates that the C_6H_6 molecule may rapidly shuttle between the two ends of the cavity of **1**.

These results can be compared to results reported in the literature for the binding of benzene by cucurbit[n]urils. For example, Kim and co-workers have determined that CB[6] binds only weakly to benzene with $K = 27$ M^{-1}.[35] These values of K represent $\Delta G°$ of inclusion values of −27.1 and −8.1 kJ mol^{-1}, respectively, for benzene in **1** and CB[6], respectively (assuming $T = 22$ °C in each case). Thus, cucurbit[6]uril analogue **1** is a much better host for benzene binding it 250-fold more tightly than CB[6]. This may be partly a result of a better matching of the size and shape of benzene with the cavity of **1** relative to CB[6]. More importantly, however, is the possibility for $\pi-\pi$ interactions between the benzene ring and the electron-deficient

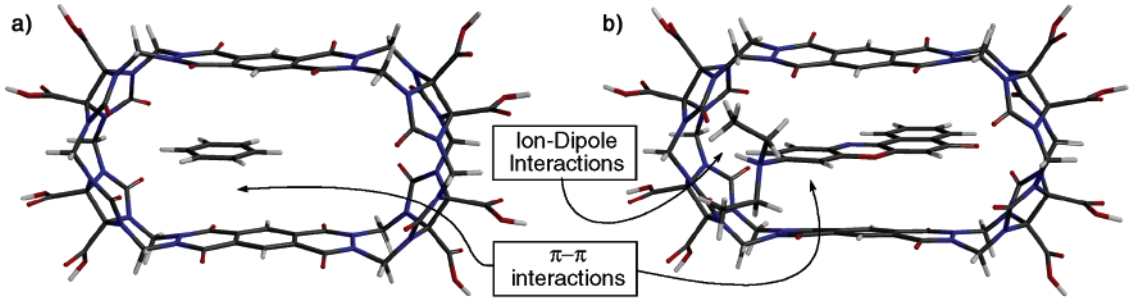

Figure 5. Minimized geometries for (a) **1**·C_6H_6 and (b) **1**·Nile Red·H^+ obtained from molecular mechanics calculations.

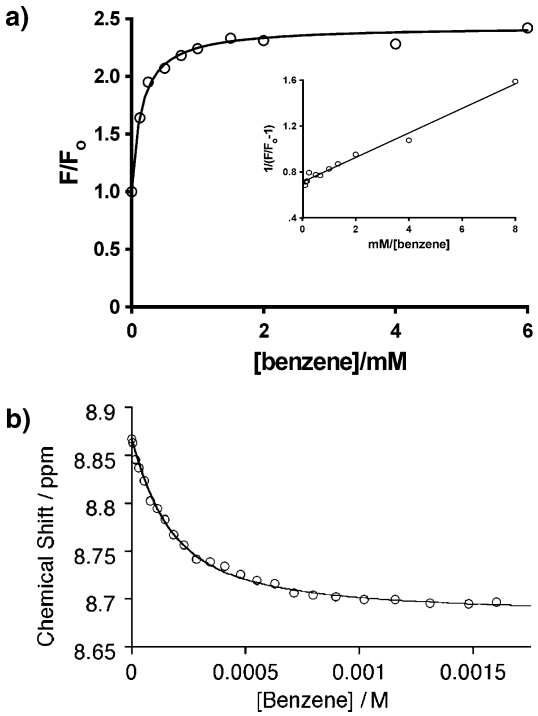

Figure 6. (a) Fluorescence enhancement of the fluorescence of a 25 μM solution of **1** as a function of added benzene; the solid line shows the best fit of the data to eq 1: $K = 6700\ M^{-1}$, $F_\infty/F_o = 2.43$. The inset shows the linear double reciprocal plot. (b) A plot of chemical shift (o, Ar−H) versus [benzene] obtained by the ^{1}H NMR titration ([**1**] = 100 μM).

bis(phthalhydrizide) walls, which are not possible for CB[6] itself. This results in an increase in the strength of the host−guest interactions for benzene in **1** as compared to CB[6], resulting in the observed much more strongly bound inclusion complex.

3.3. Effect of Inclusion into Cucurbit[6]uril Analogue 1 on Nile Red Fluorescence. As can be seen in Figure 3, the absorption of **1** is negligible above 450 nm; this allows for the study of the inclusion of polarity sensitive fluorescence probes as guests, as long as they absorb above this wavelength. Nile Red is one such fluorescent probe; it exhibits highly polarity sensitive fluorescence,[36−39] with an absorption maximum at ca. 540 nm. It has proven to be a useful fluorescent probe for the study of supramolecular inclusion systems, including micelles[40−42] and cyclodextrins.[43−45]

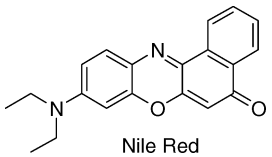

Nile Red

Nile Red has a very low aqueous solubility. However, this can actually be taken advantage of in investigating host properties: if a host is able to include Nile Red, this will significantly increase the solubility of Nile Red; this can be conveniently measured using absorption spectroscopy. Figure 7a shows the absorption spectrum of saturated Nile Red solutions containing various hosts, including **1**, CB[6], and hydroxypropyl-β-cyclodextrin (HP-β-CD), in the region of 400−700 nm, where absorption is due only to Nile Red. As can be seen, the cucurbit[6]uril analogue **1** provides the greatest increase in Nile Red solubility, indicating that it forms the strongest complex with this guest. In fact, it is the only host which solubilizes Nile Red enough to allow its absorption spectrum to be measured in acetate buffer. Figure 7b shows the fluorescence spectrum of these saturated solutions. Interestingly, the cucurbit[6]uril analogue **1** solution, which showed an extremely large Nile Red absorption relative to the other two hosts, shows a Nile Red fluorescence spectrum only about twice as large as that in HP-β-CD. This suggests that the Nile Red is much less fluorescent in the cucurbit[6]uril analogue **1** solution than in HP-β-CD solution. CB[6] shows no measurable effect on Nile Red fluorescence or solubility.

The effect of **1** on Nile Red fluorescence can be studied directly, since a relatively strong fluorescence spectrum can be obtained from a saturated solution of Nile Red in acetate buffer in the absence of host, as shown in Figure 8a. Upon addition of **1**, this fluorescence was significantly suppressed, as suggested by the results described above, even at μM levels of **1** (indicating an extremely high binding constant). This fluorescence suppression of Nile Red upon titration with **1** is shown in Figure 8b−d. There is also a significant accompanying red-shift of the position of the emission maximum from 652 to 665 nm. This decrease in intensity and red-shifting observed upon inclusion into **1** is opposite to what would be expected on the basis of the trends reported for the solvent polarity dependence of Nile Red, namely, a significant blue-shift in the spectrum (comparing methanol to water, for example)[37] and a significant increase in fluorescence quantum yield ($\phi_F = 0.29$ in acetonitrile and 0.08 in methanol)[39] upon decreased solvent polarity. The cavity of **1** is clearly less polar than water; this hydrophobic nature is part of the driving force for inclusion of hydrophobic guests such as benzene and Nile Red.

The sensitivity of Nile Red fluorescence to solvent polarity is a result of polarity effects on the formation of a twisted intramolecular charge transfer (TICT) state from the initially excited state.[38,39,41−43,45] Formation of the TICT state involves rotation of the diethylamino side group relative to the planar fused aromatic rings; electron transfer from the diethylamino group to the aromatic rings results in a zwitterionic structure. Interestingly, in polar media only the initially excited state is fluorescent, and formation of the nonfluorescent TICT state represents the major nonradiative decay path in Nile Red.[38,45]

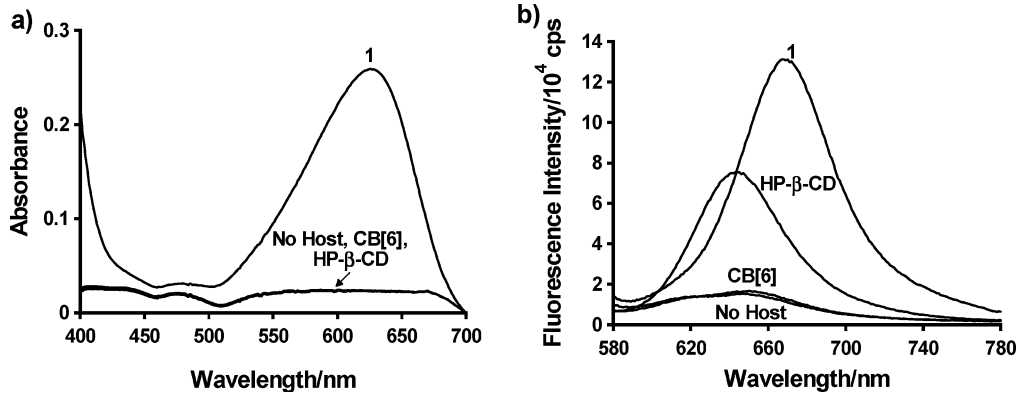

Figure 7. (a) Absorption and (b) fluorescence spectra of saturated Nile Red (structure shown in a) in various 120 μM host solutions.

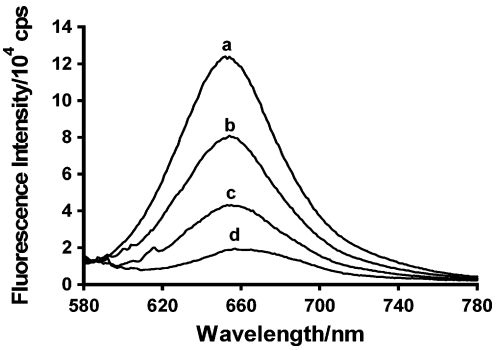

Figure 8. Fluorescence spectrum of Nile Red (structure shown) in the (a) absence and (b−d) presence of **1**: (b) 0.10 μM; c: 0.40 μM; d: 10 μM.

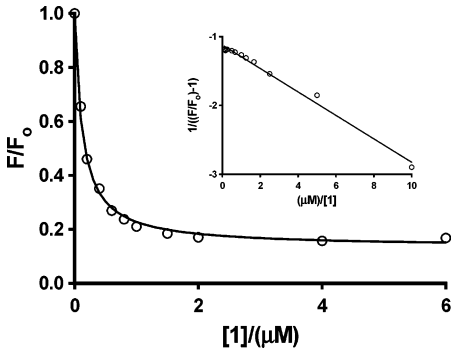

Figure 9. Fluorescence suppression of Nile Red fluorescence as a function of added host **1**; the solid line shows the best fit of the data to eq 1: $K = 8.2 \times 10^6$ M^{-1} and $F_\infty/F_o = 0.13$. The inset shows the linear double reciprocal plot.

TICT formation is enhanced in higher polarity solvents or environments, resulting in a lower fluorescence quantum yield and a red-shift in the emission spectrum.

As observed by Marquez and Nau,[46] the pK_a of CB[6] complexed amines increases by approximately 1 pK_a unit; we therefore suspect that Nile Red may be protonated within this CB[6] analogue at pH 4.74. Figure 5b shows the geometry calculated for **1**·Nile Red·H$^+$; the diethylammonium group is twisted to maximize ion−dipole interactions and to minimize unfavorable steric interactions of the Et groups with the host.

Thus, the effect of inclusion into **1** on Nile Red fluorescence is not a reflection of the local polarity changes, which would predict an *increase* in Nile Red fluorescence in the relatively nonpolar host cavity. It is also not an effect of inclusion into the restrictive environment of the cavity of **1**, since again this would result in a decrease in TICT formation (because of hindered rotation of the diethylamino group) and thus an *increase* in Nile Red fluorescence. Rather, the observed decrease in the Nile Red fluorescence must be a result of a direct effect of the cavity on the TICT process, resulting in its enhancement. This can be envisioned as a result of ion−dipole interaction between the cation part of the TICT zwitterion (the diethylamino group) and the host. Such interaction would stabilize the TICT state, resulting in an increase in its rate of formation and thus an increase in the nonradiative decay of the initially excited fluorescent state, resulting in the observed decrease in fluorescence quantum yield (intensity) and red-shifted emission. It is also possible that the expected protonation of Nile Red complexed in the cavity of **1**, as illustrated in Figure 5b, could in itself be responsible for the observed decrease in fluorescence.

These results are in direct contrast to those reported for Nile Red in cyclodextrins, in which enhanced, blue-shifted fluorescence was observed upon formation of 1:1 inclusion complexes,[44,45] attributed both to the decreased polarity of the cyclodextrin cavities[44,45] and to restricted rotation of the diethylamino group in Nile Red.[45] This illustrates the significant differences in the nature of the cavity in **1** compared to that in cyclodextrins.

Such a case of fluorescence suppression, as opposed to fluorescence enhancement, can also be treated using eq 1.[47] The only difference is that in this case, F/F_o values are *less* than 1.0. The results of a fluorescence titration of Nile Red with **1** is shown in Figure 9. The inset shows the linear double reciprocal plot ($r = 0.994$), indicating the formation of a 1:1 host:guest inclusion complex. The solid line in Figure 9 shows the excellent fit of the data to eq 1, with $K = 8.2 \times 10^6$ M^{-1} and $F_\infty/F_o = 0.13$. Three such trials were performed, yielding the average values of $K = 8.2 \pm 0.5 \times 10^6$ M^{-1} and $F_\infty/F_o = 0.15 \pm 0.02$.

As in the case of benzene as guest, **1** is a much better host for Nile Red than CB[6]. As can be seen from Figure 7, CB[6] does not enhance the solubility of Nile Red measurably, nor does it affect its fluorescence spectrum. This is an even greater difference than was the case for benzene and in this case is mainly due to the elongated cavity of **1**. Nile Red is clearly too large to be included in the small, spherical CB[6] cavity, especially considering the very narrow portal of 4 Å. However, the oval-shaped cavity of **1**, with a height of 5.90 Å and a width of 11.15 Å, is of the proper dimensions to allow for complexation of Nile Red (which has a length of 10 Å and a width of 7 Å[37]). The extremely high binding constant observed ($K = 8.2 \times 10^6$ M^{-1}) corresponds to a very large $\Delta G°$ of inclusion of -39 kJ mol^{-1}. If this is an enthalpy-driven inclusion process (which will have to be investigated using temperature-dependent binding studies), then this indicates extremely strong interactions between the host and guest. This is undoubtedly partly due to the wide range of interactions expected between

these two molecules, namely, ion−dipole and $\pi-\pi$ interactions. The interactions are much stronger than those reported for Nile Red in γ-cyclodextrin, where $\pi-\pi$ interactions are not possible. For example, the K values for the 2:1 γ-CD:Nile Red complex are K_1 (i.e., the binding constant for 1:1 complexation) = 30 M^{-1}, and K_2 (binding by the second host) = 272 M^{-1}, giving an overall binding constant of 8200 M^{-2}.

4. Conclusions

In this work, we have demonstrated that cucurbit[6]uril analogue **1** is a versatile host whose recognition properties complement those of the known CB[n]. The intrinsic fluorescence of **1**, which is sensitive to guest inclusion, provides an additional means for studying its host properties using the extremely sensitive technique of fluorescence spectroscopy. In fact, native host fluorescence allows studies of *nonfluorescent guests*, which is not possible for underivatized members of either the CB[n] or cyclodextrin family of macrocycles. We have also demonstrated that, at least in the case of the two guests studied, cucurbit[6]uril analogue **1** is a significantly tighter binding host than CB[6]. This is true both for a very small guest (benzene) and a relatively large one (Nile Red): in both cases, **1** formed much stronger inclusion complexes than those reported in the literature with CB[6]. This indicates that the oval-shaped cavity and opening in **1** are quite conducive to allowing for the inclusion of guest molecules. In addition, the fact that $\pi-\pi$ host−guest interactions are possible in the case of aromatic guests results in significantly stronger binding. In fact, cucurbit-[6]uril analogue **1** is a better host for these two guests than even the widely used cyclodextrins, in this case mainly a result of additional host−guest interactions, namely, $\pi-\pi$ interactions. The fact that cucurbit[6]uril analogue **1** exhibits guest-sensitive fluorescence, combined with the fact that it shows extremely strong guest binding (including the potential for $\pi-\pi$ interactions with aromatic guests), makes it a potentially widely applicable host for the design of fluorescent molecular sensors.

Acknowledgment. B.D.W. thanks the Natural Sciences and Engineering Research Council of Canada (NSERC) for provision of financial support through a Discovery Grant as well as the Canada Foundation for Innovation, The Atlantic Canada Opportunities Agency, and the Madame Levesque Foundation for financial support for equipment. P.G.B. thanks the Natural Sciences and Engineering Research Council of Canada (NSERC) for provision of financial support through an Undergraduate Summer Research Award. L.I. thanks the National Institutes of Health (GM61854) for financial support. L.I. is a Cottrell Scholar of Research Corporation.

References and Notes

(1) Freeman, W. A.; Mock, W. L.; Shih, N. Y. *J. Am. Chem. Soc.* **1981**, *103*, 7367−7368.
(2) Mock, W. L.; Shih, N.-Y. *J. Org. Chem.* **1983**, *48*, 3618−3619.
(3) Mock, W. L.; Shih, N.-Y. *J. Am. Chem. Soc.* **1988**, *110*, 4706−4710.
(4) Mock, W. L.; Shih, N. Y. *J. Am. Chem. Soc.* **1989**, *111*, 2697−2699.
(5) Buschmann, H.-J.; Jansen, K.; Meschke, C.; Schollmeyer, E. *J. Solution Chem.* **1998**, *27*, 135−140.
(6) Buschmann, H.-J.; Schollmeyer, E. *J. Inclusion Phenom. Mol. Recognit. Chem.* **1997**, *29*, 167−174.
(7) Whang, D.; Jeon, Y.-M.; Heo, J.; Kim, K. *J. Am. Chem. Soc.* **1996**, *118*, 11333−11334.
(8) Whang, D.; Kim, K. *J. Am. Chem. Soc.* **1997**, *119*, 451−452.
(9) Whang, D.; Heo, J.; Kim, C.-A.; Kim, K. *Chem. Commun.* **1997**, 2361−2362.
(10) Lagona, J.; Fettinger, J. C.; Isaacs, L. *Org. Lett.* **2003**, *5*, 3745−3747.
(11) Mock, W. L.; Shih, N.-Y. *J. Org. Chem.* **1986**, *51*, 4440−4446.
(12) Hoffmann, R.; Knoche, W.; Fenn, C.; Buschmann, H.-J. *J. Chem. Soc., Faraday Trans.* **1994**, *90*, 1507−1511.
(13) Meschke, C.; Buschmann, H.-J.; Schollmeyer, E. *Thermochim. Acta* **1997**, *297*, 43−48.
(14) Buschmann, H.-J.; Cleve, E.; Schollmeyer, E. *Inorg. Chim. Acta* **1992**, *193*, 93−97.
(15) Buschmann, H.-J.; Jansen, K.; Schollmeyer, E. *Thermochim. Acta* **1998**, *317*, 95−98.
(16) Neugebauer, R.; Knoche, W. *J. Chem. Soc., Perkins Trans. 2* **1998**, 529−534.
(17) Wagner, B. D.; MacRae, A. I. *J. Phys. Chem. B* **1999**, *103*, 10114−10119.
(18) Wagner, B. D.; Fitzpatrick, S. J.; Gill, M. A.; MacRae, A. I.; Stojanovic, N. *Can. J. Chem.* **2001**, *79*, 1101−1104.
(19) Wagner, B. D.; Stojanovic, N.; Day, A. I.; Blanch, R. J. *J. Phys. Chem. B* **2003**, *107*, 10741−10746.
(20) Rankin, M. A.; Wagner, B. D. *Supramol. Chem.* **2004**, *16*, 513−519.
(21) Jun, S. I.; Lee, J. W.; Sakamoto, S.; Yamaguchi, K.; Kim, K. *Tetrahedron Lett.* **2000**, *41*, 471−475.
(22) Jon, S. Y.; Selvapalam, N.; Oh, D. H.; Kang, J.-K.; Kim, S.-Y.; Jeon, Y. J.; Lee, J. W.; Kim, K. *J. Am. Chem. Soc.* **2003**, *125*, 10186−10187.
(23) Buschmann, H.-J.; Wolff, T. *J. Photochem. Photobiol., A* **1999**, *121*, 99−103.
(24) Marquez, C.; Huang, F.; Nau, W. M. *IEEE Trans. Nanobiosci.* **2004**, *3*, 39−45.
(25) Smithrud, D. B.; Diederich, F. *J. Am. Chem. Soc.* **1990**, *112*, 339−343.
(26) Forman, J. E.; Marsh, R. E.; Schaefer, W. P.; Dougherty, D. A. *Acta Crystallogr.* **1993**, *B49*, 892−896.
(27) Abe, H.; Mawatari, Y.; Teraoka, H.; Fujimoto, K.; Inouye, M. *J. Org. Chem.* **2004**, *69*, 495−504.
(28) Eaton, D. F. *J. Photochem. Photobiol., B: Biol.* **1988**, *2*, 523−531.
(29) Ware, W. R.; James, D. R.; Siemiarczuk, A. *Rev. Sci. Instrum.* **1992**, *63*, 1710−1716.
(30) Phillips, D.; Salisbury, K. In *Spectroscopy*,; Straughan, B. P., Walker, S., Eds.; John Wiley & Sons: New York, 1976; Vol. 3, Chapter 5.
(31) Muñoz de la Peña, A.; Salinas, F.; Gómez, M. J.; Acedo, M. I.; Sánchez Peña, M. *J. Inclusion Phenom. Mol. Recognit. Chem.* **1993**, *15*, 131−143.
(32) Nigam, S.; Durocher, G. *J. Phys. Chem.* **1996**, *100*, 7135−7142.
(33) Fabbrizzi, L.; Faravelli, I.; Francese, G.; Licchelli, M.; Perotti, A.; Taglietti, A. *Chem. Commun.* **1998**, 971−972.
(34) Nelissen, H. F. M.; Schut, A. F. J.; Venema, F.; Feiters, M. C.; Nolte, R. J. M. *Chem. Commun.* **2000**, 577−578.
(35) Jeon, Y.-M.; Kim, J.; Whang, D.; Kim, K. *J. Am. Chem. Soc.* **1996**, *118*, 9790−9791.
(36) Greenspan, P.; Fowler, S. D. *J. Lipid Res.* **1985**, *26*, 781−789.
(37) Sackett, D. L.; Wolff, J. *Anal. Biochem.* **1987**, *167*, 228−234.
(38) Sarkar, N.; Das, K.; Nath, D. N.; Bhattacharyya, K. *Langmuir* **1994**, *10*, 326−329.
(39) Dutta, A. K.; Kamada, K.; Ohta, K. *J. Photochem. Photobiol., A: Chem.* **1996**, *93*, 57−64.
(40) Daban, J.-R.; Samsó, M.; Barolomé, S. *Anal. Biochem.* **1991**, *199*, 162−168.
(41) Datta, A.; Mandal, D.; Pal, S. K.; Bhattacharyya, K. *J. Phys. Chem. B* **1997**, *101*, 10221−10225.
(42) Krishna, M. M. G. *J. Phys. Chem. A* **1999**, *103*, 3589−3595.
(43) Srivatsavoy, V. J. P. *J. Lumin.* **1999**, *82*, 17−23.
(44) Wagner, B. D.; Stojanovic, N.; LeClair, G.; Jankowski, C. K. *J. Inclusion Phenom. Macrocyclic Chem.* **2003**, *45*, 275−283.
(45) Hazra, P.; Chakrabarty, D.; Chakraborty, A.; Sarkar, N. *Chem. Phys. Lett.* **2004**, *388*, 150−157.
(46) Marquez, C.; Nau, W. M. *Angew. Chem., Int. Ed.* **2001**, *40*, 3155−3160.
(47) Wagner, B. D.; Fitzpatrick, S. J.; McManus, G. J. *J. Inclusion Phenom. Macrocyclic Chem.* **2003**, *47*, 187−192.